Multi-robot and task-space force control with quadratic programming

Karim Bouyarmane, Joris Vaillant, Kevin Chappellet, Abderrahmane Kheddar

Multi-robot and task-space force control with quadratic programming

Karim Bouyarmane, *Member, IEEE*, Joris Vaillant, Kévin Chappellet, and Abderrahmane Kheddar, *Senior Member, IEEE*

***Abstract*—We extend the task-space multi-objective controllers that write as quadratic programs (QP) to handle multi-robot systems as a single centralized control. The idea is to assemble all the 'robots' models and their interaction task constraints into a single QP formulation. By multi-robot we mean that whatever entities a given robot will interact with (solid or articulated systems, actuated or not or partially, fixed-base or floating-base), we model them as robots and the controller computes the state of the overall system and their interaction forces in a physically consistent way. By doing so, the tasks specification simplifies substantially. At the heart of the interactions between the systems is the contact forces: we provide methodologies to achieve reliable force tracking with our multi-robot QP controller. The approach is assessed with a large panel of experiments on real complex robotic platforms (full-size humanoid, dexterous robotic hand, fixed-base anthropomorphic arm), performing whole-body manipulation, dexterous manipulation and robot-robot co-manipulation of rigid floating objects and articulated mechanisms such as doors, drawers, boxes, or even smaller mechanisms such as a spring-loaded click pen. The implementation code of the controller is made available in open source[1].**

***Index Terms*—multi-robot control, task specification, humanoid robot manipulation, manipulation force control, robot-robot co-manipulation.**

I. Introduction

TASK-SPACE sensory control [1] has reached a considerable level of maturity and implementations in kinematics and inverse dynamics [2], [3]. It was ported in a large variety of robots, especially redundant ones [4], [5], achieving multi-objective complex tasks under various constraints.

Recent implementations formulate the task-space control as a quadratic program (QP) where multiple objective tasks are ordered by means of a weighted, a strict, or a hybrid strict-weighted priority. The controller reduces to a QP solver for a problem that is built on-line, at each control loop, e.g. [6]–[10], and where the tasks are expressed as a part of the QP cost function or part of its constraints, e.g. [11], [12].

In our previous work [13], [14] we have devised a multi-contact *planner* that considers robots and objects as multi-robot systems. It also gathered non-gaited locomotion and manipulation in a single multi-contact planning framework. However, we had not proposed a *controller* that can deal with the generated plans, nor had we experimented such a common ground planning on a real robot. We propose to extend the QP control methods to encompass the idea that other objects and entities can be integrated as parts of a single controller when they come to interact with the robot. We have already proven its applicability in graphic animation of avatars [15]. We believe that this idea will be largely adopted in robotics as (i) it is easy to implement –we also provide the software implementation of the proposed framework in open-source– and (ii) it allows to ease task specification to its simplest expression, i.e. at the level of interactions. For example, when a robot has to open the fridge, our method does not ask to build specific geometric constraints [16] or virtual mechanisms [17]–[20], nor to implement a specific planning or control strategy [21]–[25]. Instead, we consider and model the fridge as a 'robot' with as many degrees of freedom as available. The user must design the fridge model (e.g. as a ROS `urdf` file) and our controller will integrate it with that of the robot and considers interaction tasks as defined through areas of interaction (contacts). The idea here is that the model already embeds the constraints (the kinematics and the dynamics ones) instead of explicitly defining them as in [26], [27].

Integrating the kinematic model of the manipulated mechanism has been proposed in previous works [23], [24]. However, they remained at the geometric level, and only the kinematics of the planned mechanisms are accounted for. The planned configurations and motions in these works do not account for the dynamics and inertia of the manipulated mechanism(s), although these will influence the robot balance through the motion. In [25] the dynamics of the articulated mechanism is accounted for, however they restrict the study to one-DoF mechanisms, and the robot balance is not an issue (manipulator), we also refer the reader to the references therein for a review of previous door and drawer opening works

Manuscript received December 31, 2016; revised Xxxxx XX, 20XX; accepted Xxxxxx XX, 20XX. Date of publication Xxxxxxxx X, 20XX; date of current version Xxxxxxxxx X, 20XX. This paper was recommended for publication by Associate Editor X. Xxxxxxxx and Editor X. XXXX upon evaluation of the reviewers comments.

This work was partially supported by the EU H2020 COMANOID project and the CNRS-AIST-AIRBUS Group Joint Research Program.

K. Bouyarmane is with Université de Lorraine, CNRS, Inria Nancy-Grand Est, Loria UMR 7503, Larsen team, Vandoeuvre-les-Nancy, France.

J. Vaillant, K. Chappellet and A. Kheddar are with the CNRS-UM LIRMM Interactive Digital Humans group, France; and the CNRS-AIST Joint Robotics Laboratory (JRL), UMI3218/RL, Japan

This paper has supplementary video downloadable material available at http://ieeexplore.ieee.org.

Color versions of one or more of the figures in this paper are available online at http://ieeexplore.ieee.org.

Digital Object Identifier 00.0000/TRO.201X.0000000

[1]Source code available on github.com/jrl-umi3218/Tasks and a more complete version on https://gite.lirmm.fr/multi-contact/mc_rtc upon request.

and their limitations. A Cartesian impedance method for the opening of a door is proposed in [21] for a mobile manipulator without balancing issues and with the door opening motion being designed for the specific task at hand.

Our controller computes desired states that have coherent contact interaction forces. Many of the intended manipulation and co-manipulation applications rely on friction (manipulation of a free-floating box for example) and necessitates to generate the right amount of normal and tangential forces. Therefore, it is important to master force control under a QP controller framework, even on position-controlled robots, which had not been previously proposed to our knowledge. Hence we propose it as another contribution of the work.

The rest of the paper is organized as follows. Section II presents the multi-robot QP formalism, with a background on QP control and an analytic case study on a minimal example system. Section III introduces QP force control to track the manipulation forces resulting from the multi-robot QP when applied on position-controlled robots. Section IV proposes a method for estimating online the inertial parameters of the manipulated objects when manipulated with the multi-robot QP. Finally, Section V presents experimentation results where our new controller is applied in very challenging scenarios involving the Kawada's HRP-4 humanoid robot, the Softbank's ROMEO arm and the Shadow's dextrous hand.

II. Multi-Robot QP

A. QP control: a brief background

QP control has been proposed in the robotics and computer graphics communities to solve the control problem of multi-body systems with floating bases subject to friction limitations. The approach appeared in particular suited for humanoid robots and humanoid virtual characters that typically feature such properties. A QP is instantiated at every control/simulation time-step minimizing the error of multiple desired task accelerations under all physical and structural constraints of the robot, which have the characteristic of being linear in the optimization vector variable composed of the control torques, contact force coefficients along the linearized friction cones, and joint accelerations. The multi-task problem is cast as a multi-objective optimization program that can be solved with a weighted-sum scalarization or a lexicographic ordering scheme, among other possible multi-objective optimization or multi-criteria decision making resolution techniques. Of the works that opted for the weigthed-sum scalarization, [28] is worth citing in the field of computer animation as one of the firsts that proposed the method for tracking in physics simulation a motion capture data clip with a standing humanoid character in a multi-contact posture. [29] enhanced the approach by accounting for bilateral grasp contact and more complex balancing strategies. [30] combined the QP controller with higher-level finite state machine and used it for locomotion with cyclic feet contact switching. [6] applied the approach for humanoid robot in acyclic multi-contact locomotion, applied later in DARPA Robotics Challenge-like scenarios in simulation in [31] and to the real robot HRP-2 climbing a vertical ladder in [12]. [32], [33] explored the continuous task activation/deactivation within this scheme by continuous variation of the weights. There are many other works that used the QP in other schemes such as force control distribution, e.g. [34]–[36]. In the following, we extend this framework to multi-contact manipulation of articulated mechanisms and floating objects by humanoids, and to multi-robot collaboration (e.g. robot-robot co-manipulation).

B. Multi-robot QP formalism

Let us consider a system of n 'robots' which can be actual robots, free-floating rigid objects, or passive articulated mechanisms such as a door, a drawer, or a valve for example. A typical minimal manipulation system would consist of $n = 2$ 'robots': the actual manipulating robot and the manipulated object or mechanism; a typical minimal collaboration system would consist of $n = 3$ 'robots': the two collaborating robots and the collaboratively manipulated object; a dexterous hand with m fingers manipulating a rigid object would consist of $n = m + 1$ 'robots', each finger and the object. We use the unified term 'robot' here to refer to all these systems since they are all instances of the general multibody model. Indeed, each of these systems $i \in \{1, \dots, n\}$ can be modeled as a fixed base or free-floating base kinematic tree structure for which the degrees of freedom (DoFs) q_i obey the following equation of motion (EoM):

$$M_i(q_i)\ddot{q}_i + N_i(q_i, \dot{q}_i) = J_i^T f_i + S_i \tau_i \,. \tag{1}$$

Equation (1) encompasses all types of robots and accounts for all underactuation possibilities (free-floating base for humanoids and for free-floating rigid objects, non-actuated joints of passive mechanisms) through the actuation-to-DoFs mapping matrix S_i. Note that we use Newton-Euler-based algorithms for the derivation of (1) in our implementation [37]. In that framework the parts of $\dot{q}_i$ and $\ddot{q}_i$ corresponding to a free-floating link (i.e. the whole object in case of a free-floating rigid object or the base link of a humanoid) are abusive notations for V_i and $\dot{V}_i$ respectively, where V_i is the $SE(3)$ velocity of the free-floating link.

The vector f_i stacks all point contact forces applied on the surfaces of robot i. These contact forces are either applied by the fixed inertial environment (e.g. at the feet of humanoids) or by another robot j (e.g. the forces applied on the hands of a humanoid by a manipulated object). The latter forces come in pairs of action/reaction forces among the system of robots according to Newton's third law, and opposite forces applied by the robot i on the robot j appear inside the vector f_j. We thus decompose the forces f_i as $f_i = (f_i^0, f_i^-, -f_i^+)$ such that f_i^0 stacks the forces applied by the fixed environment on the robot i, f_i^- stacks the forces applied by the robots $j < i$ on the robot i, and f_i^+ stacks the forces applied by the robot i on the robots $j > i$. We then denote F^0, F^-, F^+, respectively, the vectors stacking all the vectors f_i^0, f_i^-, f_i^+. Let K be the total number of forces in F^-, i.e. such that $F^- \in \mathbb{R}^{3K}$. By virtue of Newton's third law, there exists a permutation matrix $\Pi \in \mathbb{R}^{K \times K}$ such that

$$F^+ = (\Pi \otimes I_3) F^- \,, \tag{2}$$

where $\otimes$ denotes the Kronecker product. We denote $\Psi = \Pi \otimes I_3$ (itself a permutation matrix). Let K_i be the number of forces in f_i^+, i.e. such that $f_i^+ \in \mathbb{R}^{3K_i}$. The permutation matrix Ψ is decomposed into selection matrix blocks $\Psi_i \in \mathbb{R}^{3K_i \times 3K}$ in the form:

$$\Psi = \begin{pmatrix} \Psi_1 \\ \vdots \\ \Psi_n \end{pmatrix} , \tag{3}$$

such that for each i we can write $f_i^+ = \Psi_i F^-$. Finally the equations of motions (1) take the form:

$$M_i(q_i)\ddot{q}_i + N_i(q_i, \dot{q}_i) = J_{i,0}^T f_i^0 + J_{i,-}^T f_i^- - J_{i,+}^T \Psi_i F^- + S_i \tau_i \,, \tag{4}$$

where $J_{i,0}$ and $J_{i,-}$ and $J_{i,+}$ are the matrices obtained by extracting from J_i the columns corresponding to the positions of f^0, f^-, f^+ in f, respectively[2]. We stack together all the equations (4) with the following matrices and vectors

$$q = (q_1, \ldots, q_n) \,, \tag{5}$$
$$\tau = (\tau_1, \ldots, \tau_n) \,, \tag{6}$$
$$M(q) = \text{blockdiag}(M_1(q_1), \ldots, M_n(q_n)) \,, \tag{7}$$
$$J_0(q) = \text{blockdiag}(J_{1,0}(q_1), \ldots, J_{n,0}(q_n)) \,, \tag{8}$$
$$J_+(q) = \text{blockdiag}(J_{1,+}(q_1), \ldots, J_{n,+}(q_n)) \,, \tag{9}$$
$$J_-(q) = \text{blockdiag}(J_{1,-}(q_1), \ldots, J_{n,-}(q_n)) \,, \tag{10}$$
$$S = \text{blockdiag}(S_1, \ldots, S_n) \,, \tag{11}$$
$$N(q, \dot{q}) = \begin{pmatrix} N_1(q_1, \dot{q}_1)^T & \cdots & N_n(q_n, \dot{q}_n)^T \end{pmatrix}^T \,, \tag{12}$$

to get our synthetic Newton's third law-consistent EoM for the whole system of robots:

$$M(q)\ddot{q} + N(q, \dot{q}) = J_0^T F^0 + \left(J_- - \Psi^T J_+\right)^T F^- + S\tau \,. \tag{13}$$

The kinematic constraint that expresses the coincidence of the contacts points corresponding to an action/reaction pair can be synthetically written using the matrix Ψ and the principle of virtual work as

$$J_+ \dot{q} = \Psi J_- \dot{q} \,, \tag{14}$$

which is equivalent to, given that a permutation matrix is orthogonal $\Psi^T \Psi = I_{3K}$,

$$\left(J_- - \Psi^T J_+\right)\dot{q} = 0 \,. \tag{15}$$

This latter form of the constraint is consistent with the fact that F^- can be interpreted as the constraint's Lagrange multiplier in (13). This constraint has to be complemented with the fixed environment contact kinematic constraint that writes

$$J_0 \dot{q} = 0 \,, \tag{16}$$

for which F^0 also appears as the corresponding Lagrange multiplier in (13).

Note that the proposed *mathematical* Lagrange multiplier interpretations of F^- and F^0 do not oppose the fact that both F^- and F^0 consist of *physical* contact forces (as they had been initially constructed earlier in the section by concatenation of point contact forces). As a consequence of their physical nature, F^- and F^0 are indeed the correct subjects of the Coulomb friction cone constraints $F^- \in \mathcal{C}_-$ and $F^0 \in \mathcal{C}_0$ (which would not have been necessarily a justified hypothesis if we had derived (13) directly using a Lagrangian approach on the whole system made of all the robots). These friction cones are then approximated as polyhedral cones with generators stacked as columns of matrices denoted C_- and C_0 respectively. The coefficients of F^- and F^0 along the generators are denoted λ^- and λ^0 respectively, such that $F^- = C_- \lambda^-$ and $F^0 = C_0 \lambda^0$. These coefficients are constrained to be non-negative component-wise:

$$\lambda = (\lambda^-, \lambda^0) \geq 0 \,. \tag{17}$$

The constraints of the problem are completed with the appending of the joint limits, velocity limits, torque limits, and velocity-damper-based collision avoidance constraints between any links l_a and l_b, all of the initial forms

$$q_{\min} \leq q \leq q_{\max} \,, \tag{18}$$
$$\dot{q}_{\min} \leq \dot{q} \leq \dot{q}_{\max} \,, \tag{19}$$
$$\tau_{\min} \leq \tau \leq \tau_{\max} \,, \tag{20}$$
$$\dot{\text{dist}}(l_a, l_b) \geq \xi \frac{\text{dist}(l_a, l_b) - \delta_s}{\delta_i - \delta_s} \,, \tag{21}$$

where the parameters ξ, δ_i, and δ_s are explained in more details in, e.g., [12]. The constraints (18), (19) and (21) are rewritten in terms of constraints on $\ddot{q}$ as follows:

$$\frac{\dot{q}_{\min} - \dot{q}}{\Delta t} \leqq \ddot{q} \leqq \frac{\dot{q}_{\max} - \dot{q}}{\Delta t} \,, \tag{22}$$
$$\frac{q_{\min} - q - \dot{q}\Delta t}{\frac{1}{2}\Delta t^2} \leqq \ddot{q} \leqq \frac{q_{\max} - q - \dot{q}\Delta t}{\frac{1}{2}\Delta t^2} \,, \tag{23}$$
$$\ddot{\text{dist}} \geq \frac{1}{\Delta t}\left(-\xi \frac{\text{dist} - \delta_s}{\delta_i - \delta_s} - \dot{\text{dist}}\right) \,. \tag{24}$$

These formulations allow us to write the control problem for the system of robots as a single QP:

$$\min_{\ddot{q}, \tau, \lambda} \sum_{k=1}^{M} w_k ||\ddot{g}_k - \ddot{g}_k^d||^2$$
$$\text{subject to (13) (15) (16) (17) (20) (22) (23) (24)} \,, \tag{25}$$

where g_k denote the tasks (possibly multi-dimensional) and $\ddot{g}_k{}^d$ the desired task accelerations that can for example take the following form:

$$\ddot{g}_k^d = \ddot{g}_k^{\text{ref}} - P_k e_k - D_k \dot{e}_k \,, \; e_k = g_k - g_k^{\text{ref}} \,, \tag{26}$$

with P_k and D_k denoting the task gain matrices designed such that $\begin{pmatrix} 0 & I \\ -P_k & -D_k \end{pmatrix}$ is a stable (Hurwitz) matrix, and where g_k^{ref} is a reference trajectory or a fixed set-point of the task.

Once a contact state for the system of robots has been specified, the effectiveness of the formulation (25) lies in the fact that a task can be specified for any feature of any single robot or group of robots of the system. For illustration, it is sufficient to specify a task in terms of position and orientation of a free-floating manipulated object; the control commands

[2]we use the index notations $0, +, -$ in the superscript of vectors and subscript of matrices, to avoid conflict with the transpose notation of matrices

for the the manipulating robot (or the co-manipulating robots) will automatically be induced from the contact constraints through (25), without the need of explicitly specifying any task for the manipulating end-effectors. Similarly, if it is a mechanism that is being manipulated, it is sufficient to specify a task in terms of the configuration of the mechanism (opening angle of a door, rotation angle of a valve) rather than tasks for the manipulating end-effectors. As an further illustration of the expressiveness of (25), the balance of a biped robot manipulating an object with a non-negligible mass can be written in terms of a single task on the center of mass (CoM) of the whole system.

C. Interaction forces consistency with multi-robot QP: an analytic case study

By the remark at the end of the previous section, any couplings of the motions resulting from the interactions of the robots in the system are automatically accounted for in the centralized multi-robot QP (25). Such couplings cannot be handled in a straightforward and general manner by considering independent QP controllers for the robots of the system. Consider the minimal robot-robot co-manipulation system depicted in Fig 1, as an analytic study case. The system is made of two robots and one manipulated object. We suppose that the object is perfectly sliding on the floor with zero friction (or equivalently perfectly rolling on wheels without slipping).

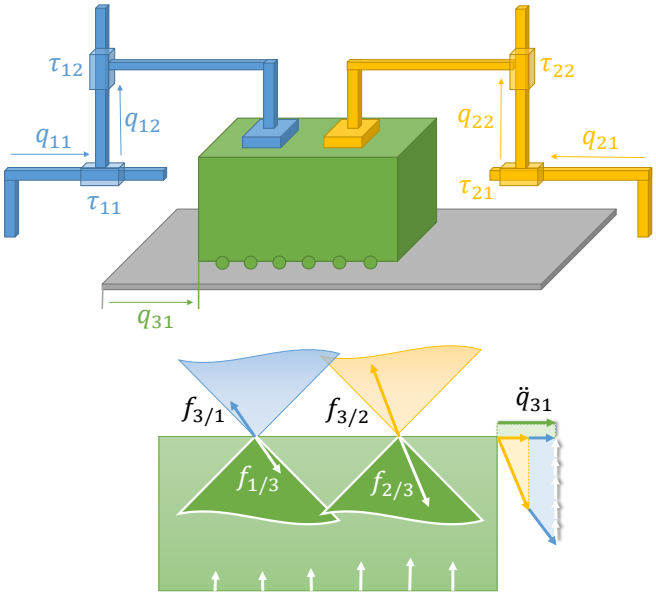

Fig. 1. Analytical example and its variables. We suppose that the manipulated object is perfectly sliding on the floor, or equivalently perfectly rolling on wheels without slipping. The object has a unit mass, so its resultant force is equal to its acceleration. We suppose that the robots links have no mass, so that the forces applied on the object are exactly equal to the actuation forces.

The objective is to bring the manipulated box from its initial state $(q_{31}, \dot{q}_{31}) = (0, 0)$ to a goal state $(q_{31}, \dot{q}_{31}) = (1, 0)$. We thus have a single 1-dimensional task $g_1(q) = q_{31}$, for which the reference value is set at $g_1^{\text{ref}} = 1$ (with $\dot{g}_1^{\text{ref}} = \ddot{g}_1^{\text{ref}} = 0$). We want a critically damped behavior for the error $e_1 = g_1 - g_1^{\text{ref}}$, so we define our desired task acceleration according to (26) as

$$\ddot{g}_1^d = -2\sqrt{1} \cdot (\dot{g}_1 - 0) - 1 \cdot (g_1 - 1) \quad (27)$$
$$= -2\dot{g}_1 - g_1 + 1\,. \quad (28)$$

We suppose that the manipulated box has a unit mass, so that

$$\ddot{q}_{31} = f_{1/3}^t + f_{2/3}^t = \tau_{11} + \tau_{21}\,, \quad (29)$$

where $f_{1/3}^t$ and $f_{2/3}^t$ are the tangential components of the forces (we denote $f_{i/j}$ the force applied by i on j). We also suppose that the robots links have no masses, so that their respective EoMs simplify to

$$\tau_1 + f_{3/1} = 0,\ \tau_2 + f_{3/2} = 0\,, \quad (30)$$

and we set the actuation limits for both τ_{11} and τ_{21} at $\tau_{\max} = 1/2$. Finally we suppose that we have a large friction coefficient (infinite).

In the following we compare a decoupled strategy consisting in solving parallel or sequential QPs for the three robots (QP1, QP2, QP3, respectively) versus one integrated multi-robot QP (QPall). Before starting with the performance comparisons, the first limitation that is immediately faced for the decoupled approach is that the unique task specification g_1 is no longer sufficient and tasks for the end-effectors of the robots 1 and 2 need to be independently specified, making sure that they are consistent with the desired object motion g_1. It is thus necessary to explicitly specify the two 2-dimensional tasks $g_1' = (g_{1x}', g_{1y}') = (q_{11}, q_{12})$ and $g_1'' = (g_{1x}'', g_{1y}'') = (q_{21}, q_{22})$ for the end-effectors of the robots 1 and 2 respectively such that $\ddot{g}_1'^d = (\ddot{g}_1^d, 0)$ and $\ddot{g}_1''^d = (\ddot{g}_1^d, 0)$.

Solving the QPs in parallel QP1 $\parallel$ QP2 $\parallel$ QP3 independently will result in the following formulation. QP1 will write as

$$\begin{aligned} \ddot{q}_{11} &= \operatorname{argmin} ||\ddot{g}_1' - \ddot{g}_1'^d||^2\,, \\ \text{subject to } & f_{3/1} + \tau_1 = 0,\ |\tau_{11}| \le 1/2\,, \end{aligned} \quad (31)$$

QP2 as

$$\begin{aligned} \ddot{q}_{21} &= \operatorname{argmin} ||\ddot{g}_1'' - \ddot{g}_1''^d||^2\,, \\ \text{subject to } & f_{3/2} + \tau_2 = 0,\ |\tau_{21}| \le 1/2\,, \end{aligned} \quad (32)$$

and QP3 as

$$\begin{aligned} \ddot{q}_{31} &= \operatorname{argmin} ||\ddot{g}_1 - \ddot{g}_1^d||^2\,, \\ \text{subject to } & \ddot{q}_{31} = f_{1/3}^t + f_{2/3}^t\,. \end{aligned} \quad (33)$$

Since $\ddot{q}_{11}$ does not appear in the EoM of (31) (because of the negligible inertia and mass hypothesis), then QP1 will mathematically output, along with the solution $\ddot{q}_{11} = 1$, any pair $(f_{3/1}, \tau_1)$ that satisfies its EoM, and for instance the solution $(\ddot{q}_{11}, f_{3/1}, \tau_1) = (1, 0, 0)$. By the symmetry of the problem the same remark goes for QP2 that will output $(\ddot{q}_{11}, f_{3/2}, \tau_2) = (1, 0, 0)$. QP3 will also output, along with $\ddot{q}_{31} = 1$, any pair $(f_{1/3}, f_{2/3})$ that satisfies its EoM, for instance $(\ddot{q}_{31}, f_{1/3}, f_{2/3}) = (1, 1/2, 1/2)$. These solutions violate Newton's third law $f_{1/3} \neq -f_{3/1}$ and $f_{2/3} \neq -f_{3/2}$.

To overcome the latter force consistency problem we can make the solution and the decision of one of the QPs available to the other QPs in a sequential scheme. Sequentially solving the QPs requires to choose an ordering for them, and in

that strategy we make QPj follow the decision of QPi for j after i in the ordering scheme, denoted QPi $\rightarrow$ QPj. In the considered example, there are 6 ordering possibilities of which only 3 need to be considered by the symmetry of the problem.

We start our analysis with the ordering QP3 $\rightarrow$ QP1 $\rightarrow$ QP2, that consists in first solving for the motion of the object then that of robot 1 then that of robot 2. QP3 will output an acceleration of the robot that is equal at $t = 0$ to

$$\ddot{q}_{31} = \text{argmin}\, ||\ddot{g}_1 - \ddot{g}_1^d||^2 = 1\,. \tag{34}$$

Feeding the output of QP3 to QP1 will produce the following set of constraints at $t = 0$

$$\ddot{q}_{11} = \ddot{q}_{31} = 1\,, \tag{35}$$
$$f_{1/3}^t = \ddot{q}_{31}\,, \tag{36}$$
$$f_{1/3}^t = \tau_{11}\,, \tag{37}$$
$$|\tau_{11}| \leq \tau_{\max} = 1/2\,, \tag{38}$$

which are not consistent (they imply $1 \leq 1/2$) since they suppose to produce a force that matches the acceleration of the object which is above the maximum actuation force. The second ordering possibility we analyze is QP1 $\rightarrow$ QP3 $\rightarrow$ QP2. This scheme encodes the strategy consisting for the robot 1 to impose a motion on the object and let robot 2 follow. QP1 will thus solve

$$\begin{aligned} \ddot{q}_{11} &= \text{argmin}\, ||\ddot{g}_1' - \ddot{g}_1'^d||^2\,, \\ \text{subject to } \ddot{q}_{11} &= \ddot{q}_{31} = \tau_{11},\ |\tau_{11}| \leq 1/2\,. \end{aligned} \tag{39}$$

The analytic expression of the solution of the differential-algebraic equation (39) is a piecewise function:

$$\ddot{q}_{11} : t \mapsto \begin{cases} \frac{1}{2}\,; & \text{if } 0 \leq t \leq \sqrt{6} - 2, \\ \frac{1}{2}\, e^{-t-2+\sqrt{6}} \Big(9 - 3\sqrt{6} + t\left(1 - \sqrt{6}\right) \Big)\,; & \text{if } t > \sqrt{6} - 2, \end{cases} \tag{40}$$

which results in the following motion of the object from QP3

$$q_{31} : t \mapsto \begin{cases} \frac{1}{4} t^2\,; & \text{if } 0 \leq t \leq \sqrt{6} - 2, \\ 1 + \frac{1}{2}\, e^{-t-2+\sqrt{6}} \Big(11 - 5\sqrt{6} + t\left(1 - \sqrt{6}\right) \Big)\,; & \text{if } t > \sqrt{6} - 2. \end{cases} \tag{41}$$

Finally QP2 will produce a motion of the robot 2 that simply follows the object by applying a zero tangential force, i.e. $f_{2/3}^t = 0$ and $\ddot{q}_{21} = \ddot{q}_{31}$ (that is, if QP2 is in some way made aware of the force already applied on the object by the robot 1, which necessitates further communication between the QPs, otherwise QP2 will output a tangential force $f_{2/3}^t = f_{1/3}^t$ which violates the EoM of the object $f_{1/3}^t + f_{2/3}^t = 2\,\ddot{q}_{31} \neq \ddot{q}_{31}$). The third and last possible ordering scheme is QP1 $\rightarrow$ QP2 $\rightarrow$ QP3 which results in the same solution and the same remarks as the previous one.

The multi-robot QP QPall however allows for a more effective collaboration since both robots will be able to apply the necessary amount of tangential force to produce an acceleration of the object that zeroes $||\ddot{g}_1 - \ddot{g}_1^d||^2$ in a consistent manner, solving the following

$$\begin{aligned} \ddot{q}_{11} &= \text{argmin}\, ||\ddot{g}_1 - \ddot{g}_1^d||^2\,, \\ \text{subject to } \ddot{q}_{11} &= \ddot{q}_{21} = \ddot{q}_{31} = f_{1/3}^t + f_{2/3}^t = \tau_{11} + \tau_{21}\,, \\ & |\tau_{11}| \leq 1/2,\ |\tau_{21}| \leq 1/2\,, \end{aligned} \tag{42}$$

that results in the following motion of the object

$$\ddot{q}_{31} : t \mapsto (1 - t)\exp(-t)\,, \tag{43}$$

i.e.

$$q_{31} : t \mapsto 1 - (1 + t)\exp(-t)\,. \tag{44}$$

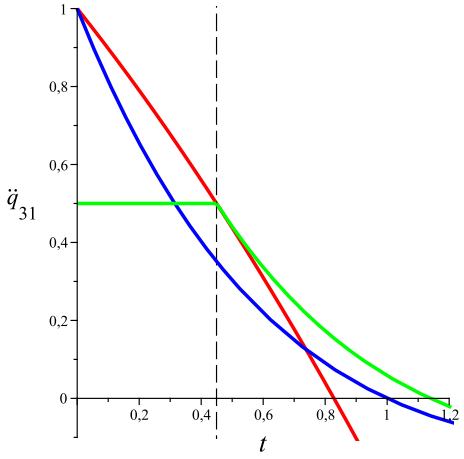

Fig. 2. In blue the resulting acceleration of the object when using the multi-robot QP QPall, in green the resulting acceleration of the object when using the decoupled strategy QP1 $\rightarrow$ QP3 $\rightarrow$ QP2, in red $\ddot{g}_1^d$ corresponding to the actuation force saturation $\tau_{11} = 1/2$ used to compute the dashed vertical line at $t = \sqrt{6} - 2$ by intersection with the horizontal line $\ddot{q}_{31} = 1/2$. In green (decoupled QPs) the acceleration of the object is saturated at the beginning of the motion due to the robots not collaborating optimally. The blue motion (multi-robot QP) is the optimal motion that zeroes $||\ddot{g}_1 - \ddot{g}_1^d||$ throughout the motion.

Fig. 2 compares the solution of QPall with the best case using decoupled QPs (QP1 $\rightarrow$ QP3 $\rightarrow$ QP2). The conclusion we can draw from this brief analytical study is twofold:

(i) decoupled QPs will in general produce non-consistent sets of constraints and forces,
(ii) even when devising adhoc strategies for a particular problem (that are not possible to generalize), a consistent decoupled strategy is less effective than an integrated one.

III. QP Force Control

The QP controller (Section II) outputs accelerations $\ddot{q}$, forces coefficients λ, and joint torques τ for the robots. We use it in our applications with position-controlled robots (Section V), by double integrating the output $\ddot{q}$ and feeding the resulting q to the low-level motor position controller. However, in view of the effective use of the multi-robot QP in interaction tasks (e.g. robots co-manipulations), it is necessary to ensure that the planned manipulation contact forces are adequately matched during the execution, even when the framework is

applied on position-controlled robots. As demonstrated in Section II-C, the formulation (25) does produce accelerations, and hence position commands, that are consistent with the *QP-predicted* contact forces λ at a given control time-step. However there are two issues with this prediction:

1) it is based on the available QP-used models of the robots and the objects, implying that any discrepancy in these models would result in non-exact predicted forces;
2) it supposes that the robot is in a given contact state that was *planned* beforehand, without actually knowing whether the robot has effectively reached that contact state and whether the contact has been established. If not, the QP would still base its calculations on the assumption that the robot is in its planned contact state and will output contact forces that are in reality null, see Fig. 3.

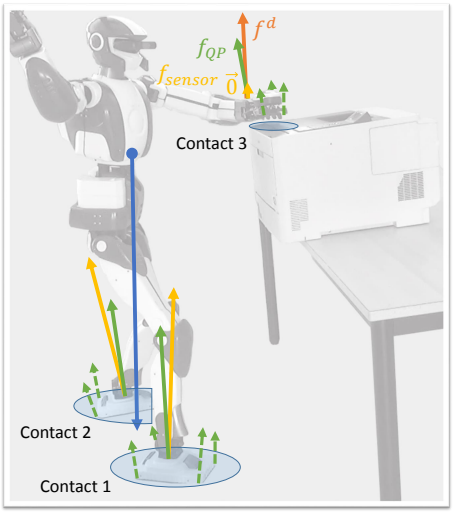

Fig. 3. Predicted forces (green) in planned contact state {Contact 1, Contact 2, Contact 3} versus sensor forces (yellow) in real contact state {Contact 1, Contact 2} (the predicted forces are resultant at the sensor locations of the point forces in dashed lines computed at the vertices of the contact prints). In this situation the QP controller assumes that the robot is in the planned contact state and therefore predicts forces that do not correspond to the actual force repartition, since the hand contact (Contact 3) is not yet established.

Therefore, we need a method to include the information from the force sensors to close the loop and realize the tracking of the predicted forces by the sensed ones. Such a closed-loop tracking method should also be able to ensure that the actual contact states match the planned ones by making sure that any planned contact has effectively been established in the current contacts state.

Force control has been extensively studied in robotics, see a thorough review in the monograhs [38], [39] and in the handbook of robotics [27]. Force control in the task space for fixed-base robots was also developed and experimented in [26], [40], [41]. Contrarily to [16], [26], task specification including force control is simplified and made straightforward with the QP built-in multi-robot constraints specification, since interaction forces are part of the QP decision variables. Active force control can be achieved either directly, through explicit closure on the force, or indirectly through impedance or admittance control [27]. The multi-robot QP control framework allows having both, and allows considering floating-base under-actuated or fixed-base robots.

To achieve force control in the multi-robot QP controller, we propose the scheme represented in Fig. 4. For a given end-effector (or more generally any link) of the robot equipped with a force/torque sensor, we proceed with an admittance controller that takes as an input the error between a target (command) force f_{target} and the corresponding sensed force f_{sensor}, and transforms it into a QP end-effector task through the following stages. First we convert the force error along the normal of the contact surface n into a velocity command with a gain (inverse of a damping) K_I (empirically set at $K_I = 5 \times 10^{-4}$ ms^{-1}N^{-1} in our applications below):

$$v = K_I \langle f_{\text{target}} - f_{\text{sensor}} | n \rangle n \,, \tag{45}$$

then we clamp that value (between $(v_{\min}, v_{\max}) = (-0.05, 0.05)$ ms^{-1} in our implementation) to prevent the end-effector from moving too fast nearby the contact surface if not reached yet (i.e. if $f_{\text{sensor}} = 0$, which happens when the end-effector is "searching" the surface it is supposed to be in contact with), this is a guarded motion with

$$v_{\text{clamp}} = \min \Big(\max \big(v_{\min}, \langle v | n \rangle \big), v_{\max} \Big) \,, \tag{46}$$

to which we apply a low-pass filter (order 3 and cutoff frequency 20Hz Butterworth in our implementation). The filtered signal $\tilde{v}$ is converted into a QP end-effector task by taking it as the reference velocity trajectory ($\dot{g}^{\text{ref}} = \tilde{v}$) and by deriving from it the reference position g^{ref} and acceleration $\ddot{g}^{\text{ref}}$ trajectories. The latter are then sent to the QP as an end-effector trajectory tracking task (here, apparent to an impedance).

We retained three possible strategies to incorporate that admittance scheme in our framework, depending on the states of the switches 1 and 2 that appear in Fig. 4. Fig. 5 illustrates a simplified representation of the different switch combinations in the block diagram of Fig. 4.

The configuration as it appears in the displayed case of Fig. 4, i.e. with switch 1 open and switch 2 up, implements an autonomous behavior where the controller tracks the force output by the QP as the QP figures it out from the other tasks of the problem. However, the user might want to have some control on interaction forces that might not turn out to be satisfactory for them (typically, in the applications and experiments of Section V, we considered that the forces output by the QP on the hands of the HRP-4 robot can be too important given the relative fragility of the hands, regardless of the nominal manufacturer's torque limits, so we wanted to produce less forces on the hand). Hence we offer the user the possibility to specify a desired force f^d that can be used in two ways. The simplest one is with switch 1 open and switch 2 down, which forces the sensor force to track f^d independently of the other physical constraints of the robot. This is not a safe strategy as the user might specify unrealistic forces f^d given the current configuration and contact state of the robot, and it can be used as a last resort only if the user is sure that the specified f^d is safe/consistent. The other way to use f^d is through the QP, with switch 1 closed and switch 2 up by

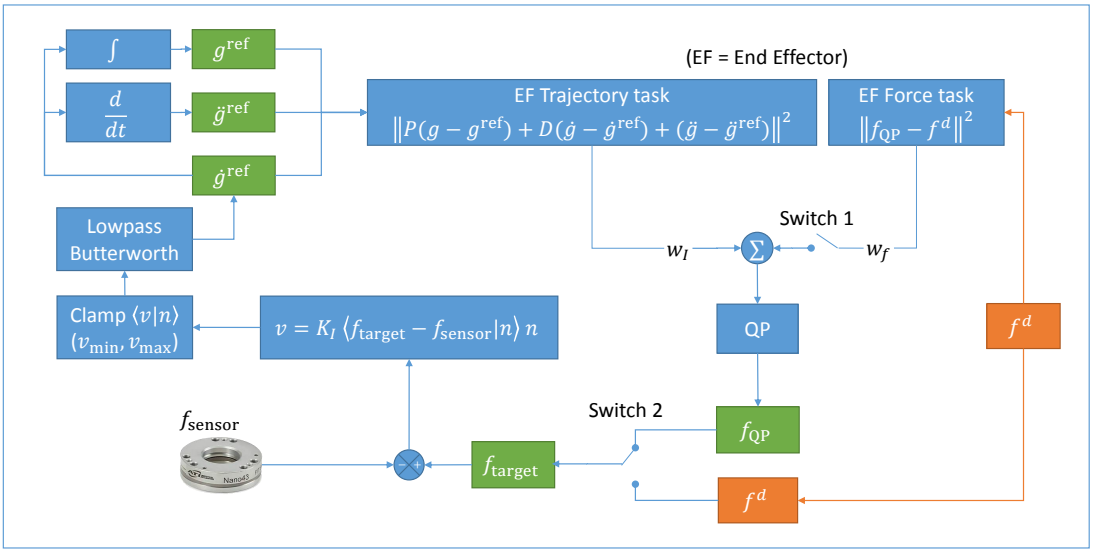

Fig. 4. Block diagram for force control with the QP. n denotes the normal vector to the contact surface, and $\langle\cdot|\cdot\rangle$ the scalar product. The error between the target force and the sensed force is converted into a velocity quantity with gain K_I then filtered with a low-pass Butterworth filter (order 3, cutoff frequency 20Hz) into a reference velocity trajectory for and end-effector standard QP trajectory tracking task. The target force comes either from the force output of the QP (switch 2 up) or from a external user command (switch 2 down). That external user command can also alternatively be incorporated inside the QP (switch 1 closed) in order to influence the force output of the QP when using the latter as a target force (i.e. with switch 2 up). In the experiments we use $K_I = 5 \times 10^{-4}$ $\text{ms}^{-1}\text{N}^{-1}$ and $(v_{\min}, v_{\max}) = (-0.05, 0.05)$ ms^{-1}.

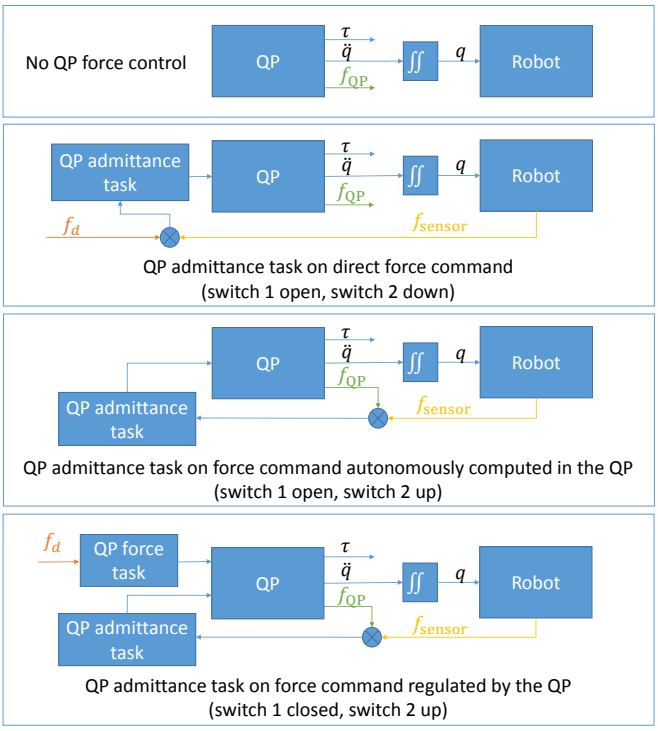

Fig. 5. Simplified representations of the different switch positions in the block diagram of Fig. 4. From top to bottom: both switches 1 and 2 open, switch 1 open and switch 2 down, switch 1 closed and switch 2 up, switch 1 closed and switch 2 down.

adding the term $||f - f^d||^2$ to the cost function of the QP, that we call a *QP force task*. This ensures that the user-specified force f^d is filtered through the physical constraints that are taken into account in the QP and produces an f_{target} that is as close as possible to f^d while remaining physically consistent.

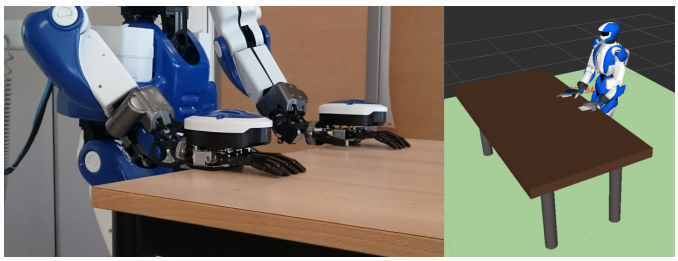

Fig. 6. Base experiment for comparing the different proposed QP force control paradigms. Each hand is controlled with a different paradigm.

Fig. 6 shows the experimental setup that was used to assess the QP force control with comparative plots in Figs. 7 and 8. The robot HRP-4 is equipped with a 6-DoF force/torque sensor at each wrist (Nano 40 from ATI). It is put near a table in a half-sitting initial posture (i.e. the knees are lightly bending). A posture is computed so that both hands are put on the table in a similar way. The force control goal is specified for each hand independently via the QP controller to press against the table.

IV. Manipulated Object Inertial Parameter Estimation

The application of the multi-robot QP approach to the particular problem of object or mechanism manipulation is based on the EoM of the manipulated object/mechanism, that appears among the EoMs concatenated in (13) and used as a constraint of (25). This is also the case in the usage of virtual mechanisms [17], [18], [20]. If the dynamics model of

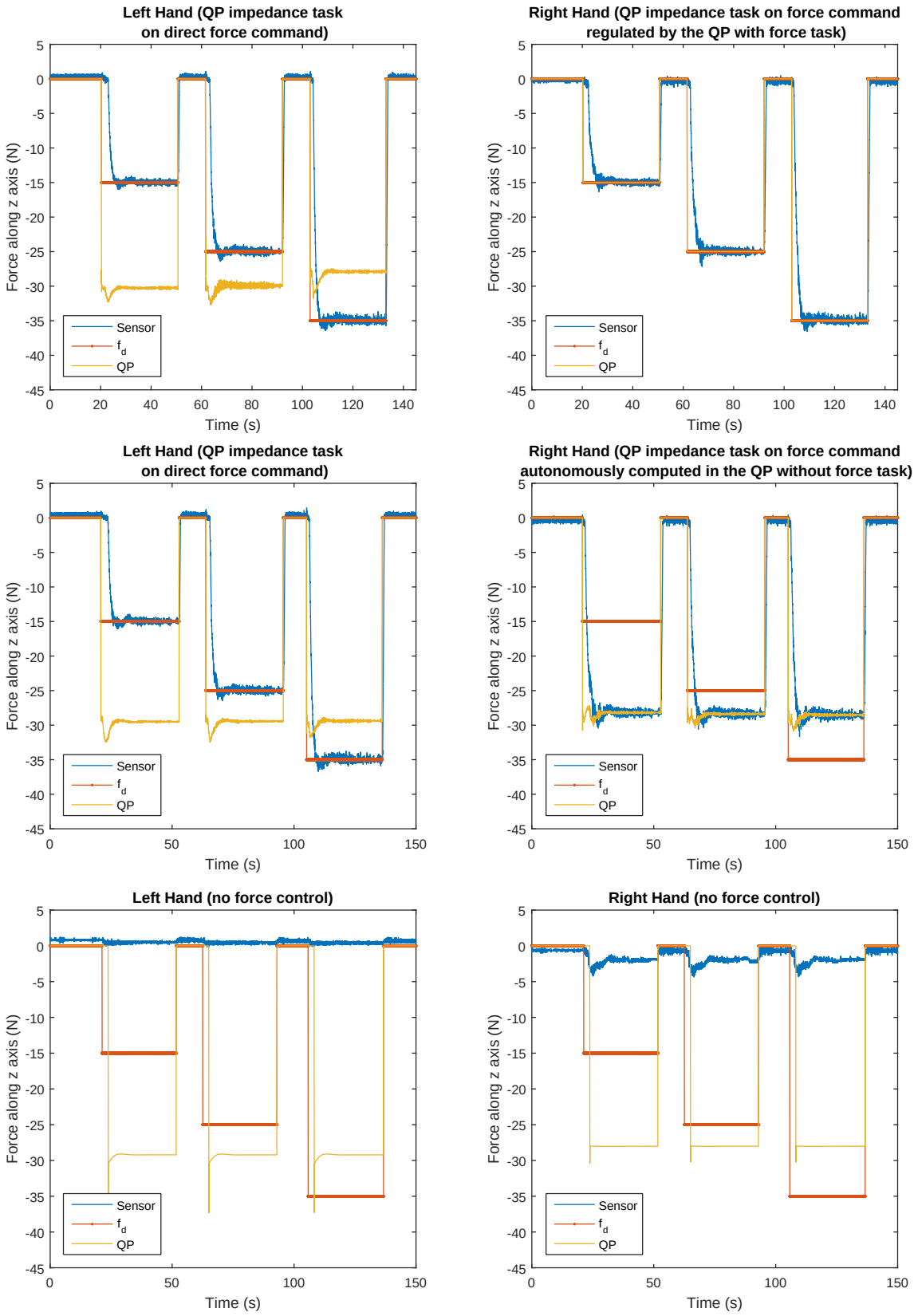

Fig. 7. Three different executions of the experiment in Fig. 6 to compare the different proposed QP force control methods. Each row represents the data for one run of the experiment.

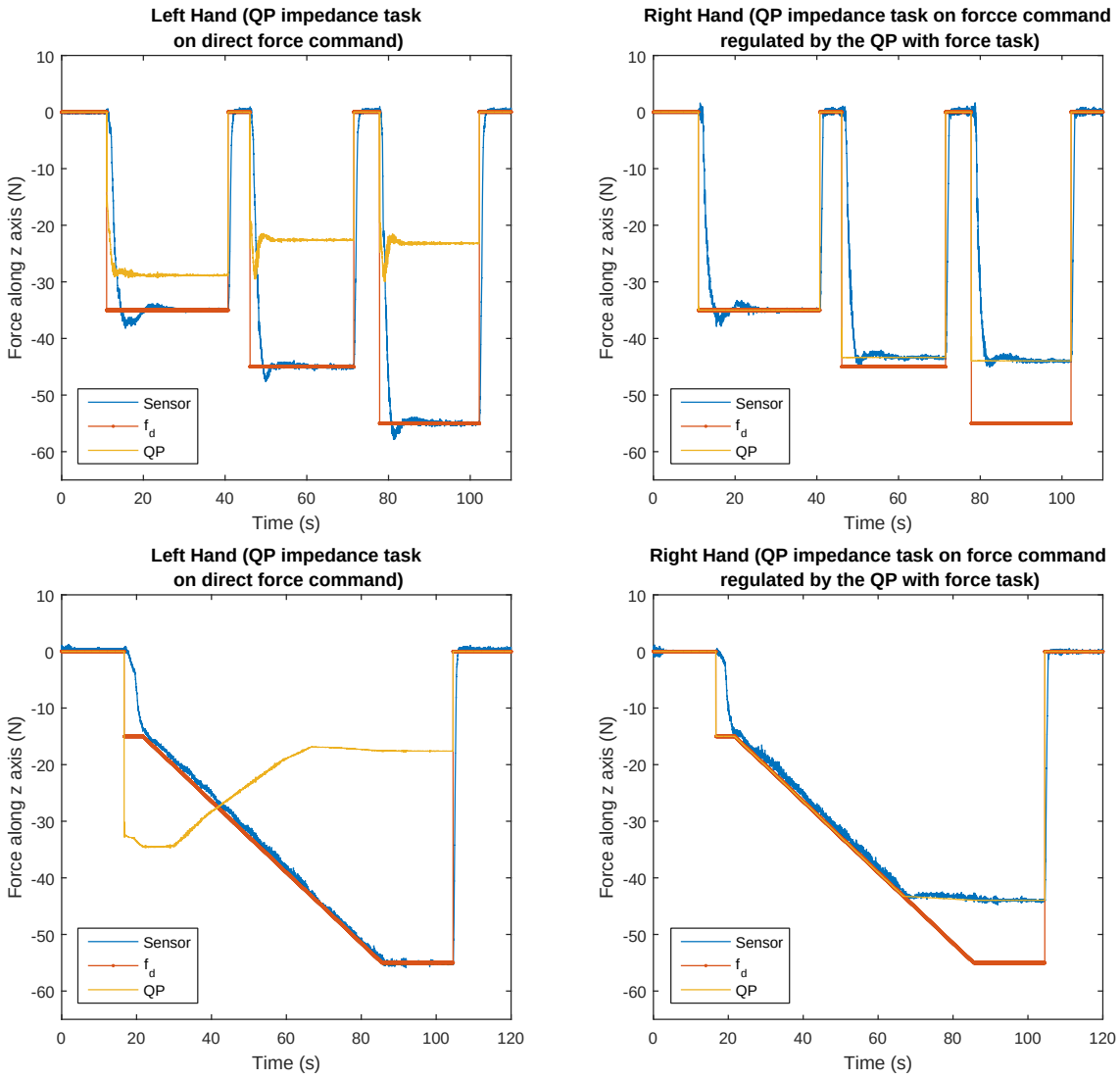

Fig. 8. Comparison between the two methods that account for a desired force command f_d, in two additional instances of the experiment in Fig. 6. In the first method, the robot follows the user command but reaches torque limits (over-torque errors appeared on the robot during both executions). The the second method (right hand), the QP autonomously "saturates" the exaggerated force command to keep the robot within the torque limit constraint. The second method is thus the safest for the robot.

the manipulated object and its inertial parameters are known, then they can be directly provided to the controller. Otherwise, the robot should "discover" them while executing the manipulation motion, adapting the motion from a very rough initial knowledge-based estimate to the real dynamic parameters as they are being estimated online [25], [41]. Although inertial parameter identification through object manipulation is not the main stream of our contribution and a large body of work already exists in robotics, we propose in this section to provide guidelines of its integration in the multi-robot QP framework, for the paper to be self-contained.

The manipulated mechanism of index i in the multi-robot system is composed of n_i links ($n_i = 1$ for a floating object without any mechanism), the inertial parameters of which are

$$\phi^{ij}_{\text{link}} = (m^{ij}, h^{ij}_x, h^{ij}_y, h^{ij}_z, I^{ij}_{xx}, I^{ij}_{xy}, I^{ij}_{xz}, I^{ij}_{yy}, I^{ij}_{yz}, I^{ij}_{zz}) , \quad (47)$$

where j is the index of the link within the mechanism, m^{ij} its mass, $(h^{ij}_x, h^{ij}_y, h^{ij}_z)$ the position of its center of mass, and $(I^{ij}_{xy}, I^{ij}_{xz}, I^{ij}_{yy}, I^{ij}_{yz}, I^{ij}_{zz})$ the entries of its inertia matrix. Additionally, we consider the cases of possibly spring-loaded joints in the manipulated mechanisms. Such a joint j of the mechanism i is subject in the EoM (1) to the torque vector component

$$\tau_{ij} = K^{ij} q_{ij} + C^{ij} \dot{q}_{ij} + O^{ij} , \quad (48)$$

where

$$\phi^{ij}_{\text{joint}} = (K^{ij}, C^{ij}, O^{ij}) , \quad (49)$$

denote respectively the stiffness, damping, and a constant offset. The inertial parameters of the mechanism i can thus be concatenated in the vector

$$\phi^i = (\phi^i_{\text{links}}, \phi^i_{\text{joints}}) , \quad (50)$$

where $\phi^i_{\text{links}} = (\phi^{ij}_{\text{link}})_{1 \leq j \leq n_i}$, and $\phi^i_{\text{joints}} = (\phi^{ij}_{\text{joint}})_{j \in J_i}$, J_i denoting the indexes of the joints of the mechanism i that have a spring-damper mechanism in them. All in all, ϕ^i is the

vector of parameters the robot needs to estimate. It is a known property that the EoM (1) is linear in the inertial parameters, i.e. that the EoM can be rewritten in the form

$$Y^i(q_i, \dot{q}_i, \ddot{q}_i)\phi^i = J_i^T f_i \,, \tag{51}$$

where $Y^i = \begin{pmatrix} Y^i_{\text{links}} & Y^i_{\text{joints}} \end{pmatrix}$ is a block matrix concatenating the matrices linearly mapping the inertial parameters of the links of the mechanism and those of its spring-loaded joints, respectively, to the generalized forces in the EoM. The parameters ϕ^i can be estimated using a least-square-based regression on a given number of samples of $(q_i, \dot{q}_i, \ddot{q}_i)$ (more precisely, we implemented an iteratively reweigthed least square (IRLS) regression). This method is however not the most suitable one for our purpose of online estimation since the identification is made after all the sample measurements have been performed. We thus prefer a method based on a discrete Kalman filter with state ϕ^i and observation $\mu^i = J_i^T f_i$ according to the model:

$$\phi^i_k = \phi^i_{k-1} + w_k \,, \tag{52}$$
$$\mu^i_k = Y^i \phi^i_k + v_k \,, \tag{53}$$

where w_k and v_k are zero-mean multivariate Gaussian distributions with covariance matrices Q and R respectively

$$w_k \sim \mathcal{N}(0, Q) \,, \;\; v_k \sim \mathcal{N}(0, R) \,. \tag{54}$$

R is obtained from force sensor calibration on the manipulating end-effector of the robot, while Q expresses our confidence in the dynamics model and we practically set it as diagonal matrix with diagonal elements orders-of-magnitude less than the diagonal elements of R_k, expressing the fact that the confidence in the model is significantly higher than the confidence in the force sensor data. Dropping in the notations the superscript i since there is no ambiguity, let $\hat{\phi}^-_k$ and $\hat{\phi}_k$ denote respectively the *a priori* and *a posteriori* estimates of the state ϕ_k, and let the corresponding *a priori* and *a posteriori* estimation errors be $e^-_k = \phi_k - \hat{\phi}^-_k$ and $e_k = \phi_k - \hat{\phi}_k$ respectively. Their respective covariance matrices are denoted $P^-_k = E[e^-_k e^{-T}_k]$ and $P_k = E[e_k e^T_k]$. The predict phase of the Kalman filter writes

$$\hat{\phi}^-_k = \hat{\phi}^-_{k-1} \tag{55}$$
$$P^-_k = P^-_{k-1} + Q \,, \tag{56}$$

and its update phase in which the optimal gain matrix L_k is computed

$$L_k = P^-_k Y^T \left(Y P^-_k Y^T + R \right)^T \,, \tag{57}$$
$$\hat{\phi}_k = \hat{\phi}^-_k + L_k \left(\mu_k - Y \hat{\phi}^-_k \right) \,, \tag{58}$$
$$P_k = (I - L_k Y) P^-_k \,. \tag{59}$$

Section V shows results for this estimation approach in an example multi-robot QP experiment.

V. Experimentations

We experimented the multi-robot QP controller on various challenging scenarios that were recorded in the accompanying video. The scenarios use three different robots: the Kawada HRP-4 humanoid robot, the Aldebaran ROMEO arm (with a hand), and the Shadow dextrous multi-finger hand.

A. Inertial parameter estimation experiment

We tested the inertial parameter estimation method proposed in Section IV in a multi-robot QP setting on a box manipulation experiment in Fig. 9. The box is modeled as a one-link free-floating robot with unknown mass and center-of-mass, only the geometric model of the box is known to the controller. The force-control scheme with autonomous QP (switch 1 open switch 2 up combination) is used to ensure that the robot applies sufficient force to avoid box slippage. The box is a cardboard filled with various arbitrary objects tightly occupying all the space inside the box (to have a constant CoM). The measured mass of the box with its content was 0.941kg. However the robot was provided with an initial estimate of 0.1kg. Fig. 10 shows the results obtained by using the presented Kalman filter method with the multi-robot QP controller. It can be seen in this example that the method quickly converges to an estimated mass of 0.947kg hence with a 0.6% relative error.

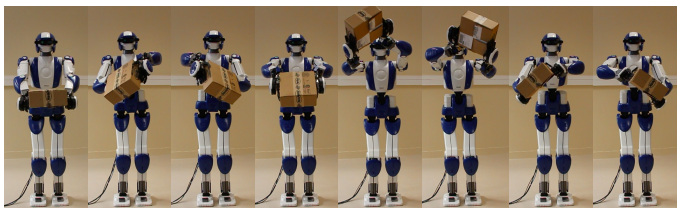

Fig. 9. Example of on-line dynamic inertial parameter estimation experiment for a manipulated box. Each image shows a posture way-point.

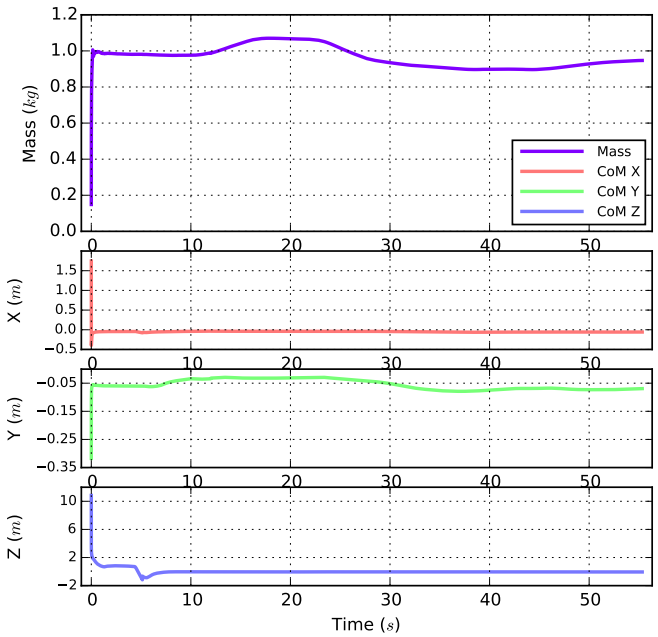

Fig. 10. Parameter estimation of the manipulated box using the Kalman filter method.

B. Manipulation of articulated mechanisms

In these experiments, we illustrate the capabilities of the controller to manipulate every-day-life objects with articulated

mechanisms. Two manipulation scenarios were experimented in this regard: door opening and printer tray opening. The robot is the HRP-4 humanoid that is provided with the `urdf` models of the objects. The door is a regular (not self-closing) door of the laboratory room intended for everyday use. It is modeled in the multi-robot QP as a 'robot' with a two-DoF fixed-base mechanism. One DoF is the passive revolute joint at the hinges of the door; the second one is a spring-loaded revolute joint at the knob of the door. The printer is a commercial printer (model Canon i-sensys LPB7680Cx). It is also modeled in the multi-robot QP as 'robot' with a fixed-base mechanism (although it could have been more accurately modeled as floating-base mechanism in unilateral contact with the support table) with one passive prismatic joint for the tray (the model can also include the other non-used trays and also all the buttons as prismatic joints).

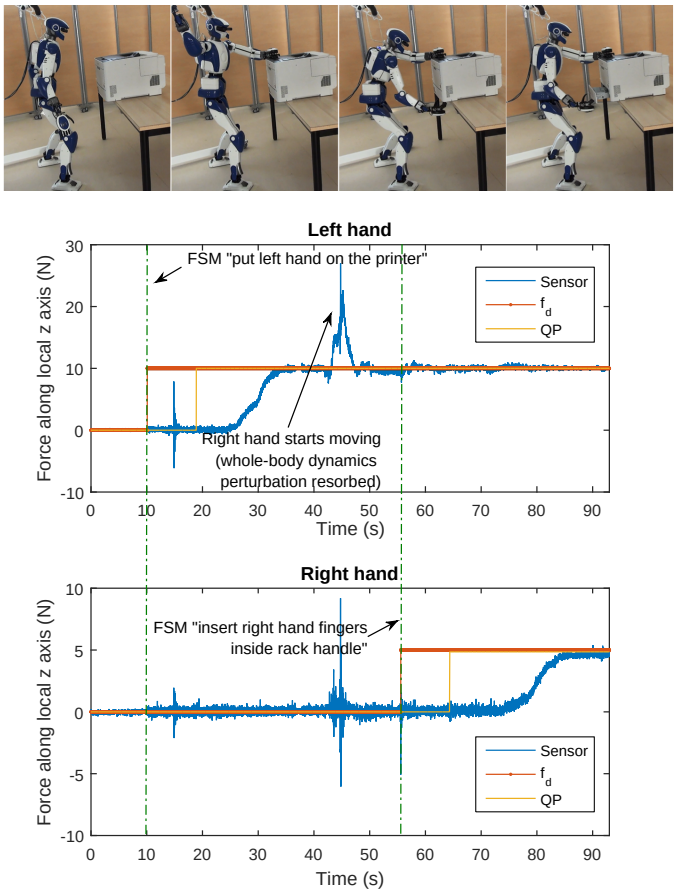

Fig. 11. Printer tray opening with HRP-4.

In the printer experiment, the user provides a desired force $f_d = 10\,\mathrm{N}$ along the local z-axis on the left hand in order to prevent its slippage (to compensate for the modeling approximation that we make consisting in defining a planar surface on the hand of HRP-4 which is not perfectly planar) and a desired force $f_d = 5\,\mathrm{N}$ along the local z-axis on the right hand to firmly insert it inside the tray handle prior to the tray pulling motion. See Fig. 11. Both force commands are sent in the "switch 1 closed, switch 2 up" combination of the controller in Fig. 4. Putting the left hand on the printer is suggested by the planner [14] to create a closed kinematic chain so as to pull the tray without problem of equilibrium or force application.

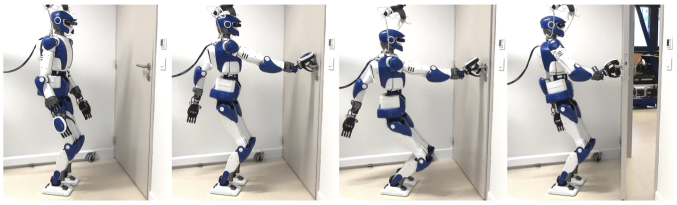

Fig. 12. Door opening with HRP-4 using the force control scheme of the multi-robot QP.

Fig. 12 illustrates snapshots from the door opening experiment with the same controller. The accompanying video shows an additional door opening experiment using a position control scheme of the knob, with another robot posture where the door is opened with the left arm, pushed with the right one and finally crossed using a walking controller [42]. This is an example of sequencing the multi-robot QP controller with other controllers such as a walking controller in this case.

C. Robot-robot co-manipulation

We experimented the multi-robot QP paradigm for actual multi-robot collaborative task between a humanoid robot ROMEO's left arm from SoftBank Robotics and the humanoid robot HRP-4. The two robots use different and unrelated low-level control and communication architectures, as well as different control frequencies (respectively 100Hz and 200Hz), constituting a challenging setting for the multi-robot QP controller.

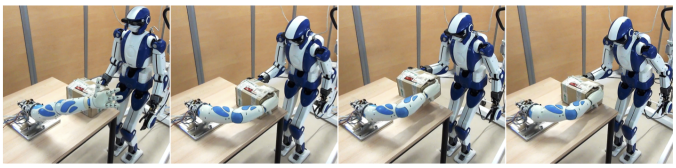

Fig. 13. Multi-robot collaborative manipulation between HRP-4 and ROMEO's left arm.

The multi-robot QP controller computations were carried on an external computer and sent to both robots using dedicated communication architectures. We plan in the future to embark the multi-robot QP control computations on one of the robots and use the other robot's computational resources for auxiliary tasks such as vision for example.

The task consisted in a collaborative pick-and-place operation, collaboratively lifting a box (a random parcel package delivered by the post containing electronics parts that were not removed from the box) and putting it down on a different location. The task was only specified in terms of positions of the box using three way points: lifting up, translating to the right (of HRP-4), putting down. When putting down we specified a slightly lower height than the lifting-up height to ensure that the contact between the box and the table is well established and avoid dropping the box from a non-zero height. This one-task specification is illustrative of the multi-robot QP

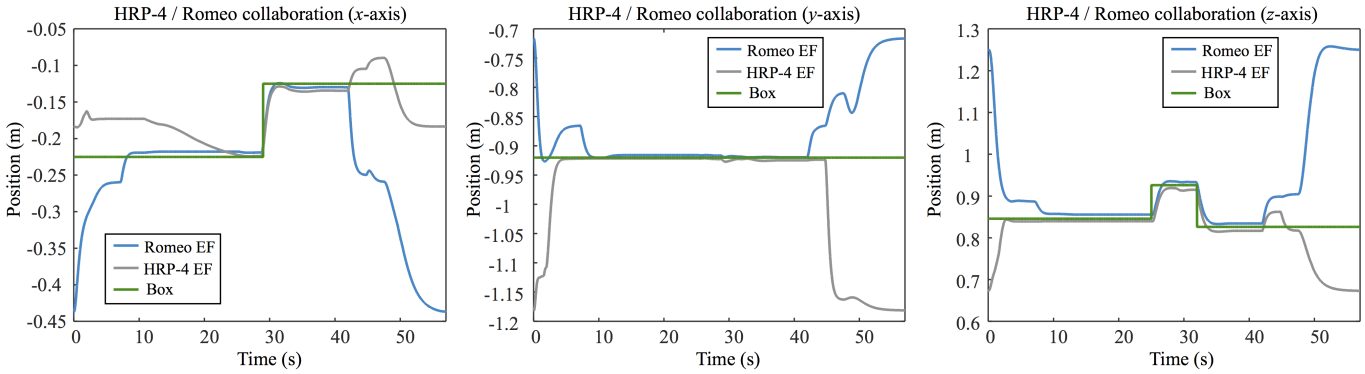

Fig. 14. Robot-robot co-manipulation motion. Resulting coordinated motion (position of HRP-4 and that of ROMEO's hand link frames) from single task command (position of box frame).

coordination capabilities, since no explicit task is needed for the hands of the two robots, the unilateral contact constraints between the hands and the box being sufficient. Force control was additionally implemented in this experiment to maintain the contact force between the HRP-4 hand and the box, and the ROMEO hand and the box. Not using the QP force control scheme resulted in the slippage of the box and the robots were not able to lift it. Fig. 14 tracks the motions of fixed points on the contact surface frames of the hands of the robots in comparison with the motion of a fixed point in the box frame representative of the task.

D. Dexterous manipulation

Both the HRP-4 and ROMEO robots are equipped with gripper mechanisms at the hand that do not implement anthropomorphic dexterous hand capabilities. We thus chose to demonstrate the multi-robot QP applicability to dexterous manipulation problems on a Shadow dexterous hand with 19 DoFs.

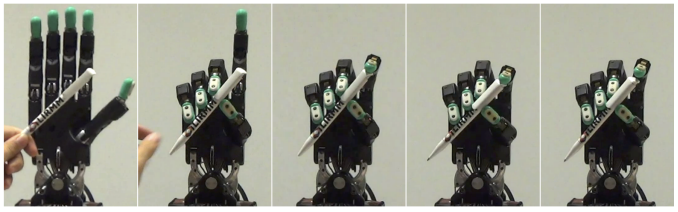

Fig. 15. Dexterous hand clicking a pen.

We chose an illustrative manipulation problem where the manipulated object, a click pen, is again an articulated mechanism, but as opposed to the door and printer it is this time a free-floating base mechanism. The cardboard boxes in the previous experiments were also free floating but without articulations. Hence with this last example we cover all typologies of manipulated objects. The clicking articulation is modeled with a spring-loaded prismatic joint in the multi-robot QP. The contact surfaces on the fingertips and the cylindrical body of the pen were faceted (approximated with planar surface patches).

The task in this example was specified on the configuration of the pen 'robot' such that the position of the clicking part reaches its joint limit to trigger the exit of the writing tip. See Figs. 15 and 16.

Fig. 16. The green spots are the predefined contact areas.

VI. Conclusion

We show the benefit of integrating task-space QP controllers as a single problem to handle multi-robot interactions. By multi-robot we mean that the controller can deal with any objects or robots or mechanisms that are passive, partially or totally actuated, with which a given robot interacts. Not only does such an approach ease the specification of the tasks (as a complement to planning) to its simplest expression (i.e. the interaction level), but it also computes physically correct contact interaction forces. Subsequently, we devised force control algorithms for QP controllers and show that we can achieve reliable closed-loop force control where the QP can track at best the desired forces (and does its best when they are not feasible). The implementation code of the multi-robot controller is provided in open source; it has been interfaced with vRep and Gazebo simulators. The code is already distributed to several teams worldwide, it is sustained, and has been implemented on other humanoid and robotic platforms (e.g. ARMAR, Nao, HRP-2Kai, KuKa arms, etc.)

QP controllers are currently emerging as a gold standard to handle multi-objective tasks in redundant robots such as humanoids. They prove capable of controlling position, torque and now multi-robots and force. Recently our controller has been enhanced with visual servoing [43] which makes it a multi-modal controller as vision, force, impedance/admittance,

and position tasks can be specified in conjunction. Thorough investigations in terms of stability have been conducted in [44].

As future work, we will enhance the perception of the multi-robot part. Namely, when interacting with objects, eventually articulated, that do not have embedded sensors to measure their configuration, and that we need to estimate using vision. We are also conducting promising research to use the QP also as an adaptive controller, where gains of the actuators [45] and the tasks are also part of the decision variables.

REFERENCES

[1] C. Samson, M. Le Borgne, and B. Espiau, *Robot control– the task function approach*. Oxford, England: Clarendon Press, 1991.

[2] N. Mansard, O. Khatib, and A. Kheddar, "A unified approach to integrate unilateral constraints in the stack of tasks," *IEEE Transactions on Robotics*, vol. 25, no. 3, pp. 670–685, 2009.

[3] L. Sentis, J. Park, and O. Khatib, "Compliant control of mult-icontact and center-of-mass behaviors in humanoid robots," *IEEE Transactions on Robotics*, vol. 26, no. 3, pp. 483–501, June 2010.

[4] Y. Nakamura, H. Hanafusa, and T. Yoshikawa, "Task-priority based redundancy control of robot manipulators," *International Journal of Robotics Research*, vol. 6, no. 2, pp. 3–15, June 1987.

[5] B. Siciliano and J.-J. E. Slotine, "A general framework for managing multiple tasks in highly redundant robotic systems," in *International Conference on Advanced Robotics*, vol. 2, Pisa, Italy, 19-22 June 1991, pp. 1211–1216.

[6] K. Bouyarmane and A. Kheddar, "Using a multi-objective controller to synthesize simulated humanoid robot motion with changing contact configurations," in *IEEE/RSJ International Conference on Intelligent Robots and Systems*, San Fransico, CA, 25-30 September 2011, pp. 4414–4419.

[7] O. Kanoun, F. Lamiraux, and P.-B. Wieber, "Kinematic control of redundant manipulators: Generalizing the task-priority framework to inequality task," *IEEE Transactions on Robotics*, vol. 27, no. 4, pp. 785–792, August 2011.

[8] P. M. Wensing and D. E. Orin, "Generation of dynamic humanoid behaviors through task-space control with conic optimization," in *IEEE International Conference on Robotics and Automation*, Karlsruhe, Germany, May 2013, pp. 3088–3094.

[9] A. Escande, N. Mansard, and P.-B. Wieber, "Hierarchical quadratic programming: Fast online humanoid-robot motion generation," *The International Journal of Robotics Research*, vol. 33, no. 7, pp. 1006–1028, 2014.

[10] S. Kuindersma, F. Permenter, and R. Tedrake, "An efficiently solvable quadratic program for stabilizing dynamic locomotion," in *IEEE International Conference on Robotics and Automation*, Hong Kong, China, 2014.

[11] S. Feng, X. Xinjilefu, W. Huang, and C. G. Atkeson, "Optimization-based full body control for the DARPA robotics challenge," *Journal of Field Robotics*, vol. 32, no. 2, pp. 293–312, March 2015.

[12] J. Vaillant, A. Kheddar, H. Audren, F. Keith, S. Brossette, A. Escande, K. Bouyarmane, K. Kaneko, M. Morisawa, P. Gergondet, E. Yoshida, S. Kajita, and F. Kanehiro, "Multi-contact vertical ladder climbing by an HRP-2 humanoid," *Autonomous Robots*, vol. 40, no. 3, pp. 561–580, March 2016.

[13] K. Bouyarmane and A. Kheddar, "Multi-contact stances planning for multiple agents," in *IEEE International Conference on Robotics and Automation*, Shanghai, China, 9-13 May 2011, pp. 5246–5253.

[14] ——, "Humanoid Robot Locomotion and Manipulation Step Planning," *Advanced Robotics*, vol. 26, no. 10, pp. 1099–1126, 2012.

[15] J. Vaillant, K. Bouyarmane, and A. Kheddar, "Multi-character physical and behavioural interactions controller," *IEEE Transactions on Visualization and Computer Graphics*, 2017.

[16] G. Borghesan, E. Scioni, A. Kheddar, and H. Bruyninckx, "Introducing geometric constraint expressions into robot constrained motion specification and control," *IEEE Robotics and Automation Letters*, vol. 1, no. 2, pp. 1140–1147, July 2016.

[17] K. Kosuge, T. Itoh, T. Fukuda, and M. Otsuka, "Tele-manipulation system based on task-oriented virtual tool," in *IEEE International Conference on Robotics and Automation*, Nagoya, Japan, 21-27 May 1995, pp. 351–356.

[18] L. D. Joly and C. Andriot, "Imposing motion constraints to a force reflecting telerobot through real-time simulation of a virtual mechanism," in *IEEE International Conference on Robotics and Automation*, Nagoya, Japan, 21-27 May 1995, pp. 357–362.

[19] A. Kheddar, "Teleoperation based on the hidden robot concept," *IEEE Transactions on Systems Man and Cybernetics, Part A*, vol. 31, no. 1, pp. 1–13, January 2001.

[20] S. A. Bowyer, B. L. Davies, and F. Rodriguez y Baena, "Active constraints/virtual fixtures: a survey," *IEEE Transactions on Robotics*, vol. 30, no. 4, pp. 138–157, February 2014.

[21] C. Ott, B. Bäuml, C. Borst, and G. Hirzinger, "Employing cartesian impedance control for the opening of a door: a case study in mobile manipulation," in *IFAC Symposium on Intelligent Autonomous Vehicles*, Toulouse, France, 2007.

[22] S. Dalibard, A. Nakhaei, F. Lamiraux, and J.-P. Laumond, "Manipulation of documented objects by a walking humanoid robot," in *IEEE-RAS International Conference on Humanoid Robots*, Nashville, TN, USA, 6-8 December 2010.

[23] D. Berenson, S. Srinivasa, and J. Kuffner1, "Task space regions: A framework for pose-constrained manipulation planning," *International Journal of Robotics Research*, vol. 30, no. 12, pp. 1435–1460, 2011.

[24] F. Burget, A. Hornung, and M. Bennewitz, "Whole-body motion planning for manipulation of articulated objects," in *IEEE International Conference on Robotics and Automation*, Karlsruhe, Germany, 6-10 May 2013, pp. 1656–1662.

[25] Y. Karayiannidis, C. Smith, F. E. V. Barrientos, P. Ögren, and D. Kragic, "An adaptive control approach for opening doors and drawers under uncertainties," *IEEE Transactions on Robotics*, vol. 32, no. 1, pp. 161–175, February 2016.

[26] H. Bruyninckx and J. De Schutter, "Specification of force-controlled actions in the "task frame formalism"– a synthesis," *IEEE Transactions on Robotics and Automation*, vol. 12, no. 4, pp. 581–589, August 1996.

[27] L. Villani and J. De Schutter, *Handbook of Robotics*. Berlin Heidelberg: Springer-Verlag, 2008, ch. Force control, pp. 161–185.

[28] Y. Abe, M. da Silva, and J. Popović, "Multiobjective control with frictional contacts," in *Eurographics/ACM SIGGRAPH Symposium on Computer Animation*, San Diego, California, 2-4 August 2007, pp. 249–258.

[29] C. Collette, A. Micaelli, C. Andriot, and P. Lemerle, "Dynamic balance control of humanoids for multiple grasps and non coplanar frictional contacts," in *IEEE/RAS International Conference on Humanoid Robots*, Pittsburgh, PA, November 29 - December 1 2007, pp. 81–88.

[30] M. de Lasa, I. Mordatch, and A. Hertzmann, "Feature-based locomotion controllers," *ACM Transactions on Graphics (SIGGRAPH)*, vol. 29, no. 4, p. 1, 2010.

[31] K. Bouyarmane, J. Vaillant, F. Keith, and A. Kheddar, "Exploring humanoid robots locomotion capabilities in virtual disaster response scenarios," in *IEEE-RAS International Conference on Humanoid Robots*, Osaka, Japan, November 2012, pp. 337–342.

[32] J. Salini, S. Barthélemy, and P. Bidaud, *LQP-based controller design for humanoid Whole-body motion*. Springer, 2010, pp. 177–184.

[33] J. Salini, V. Padois, and P. Bidaud, "Synthesis of complex humanoid whole-body behavior: A focus on sequencing and tasks transitions," in *IEEE International Conference on Robotics and Automation*, Shanghai, China, 9-13 May 2011, pp. 1283–1290.

[34] A. Herzog, L. Righetti, F. Grimminger, P. Pastor, and S. Schaal, "Balancing experiments on a torque-controlled humanoid with hierarchical inverse dynamics," in *IEEE/RSJ International Conference on Intelligent Robots and Systems*, Chicago, Illinois, 14-18 September 2014.

[35] M. Liu, A. Micaelli, P. Evrard, A. Escande, and C. Andriot, "Interactive virtual humans: A two-level prioritized control framework with wrench bounds," *IEEE Transactions on Robotics*, vol. 28, no. 6, pp. 1309–1322, December 2012.

[36] L. Righetti and S. Schaal, "Quadratic programming for inverse dynamics with optimal distribution of contact forces," in *IEEE-RAS International Conference on Humanoid Robots*, Businness Inoovation Center, Osaka, Japan, November 2012.

[37] R. Featherstone, *Rigid Body Dynamics Algorithms*. New York: Springer, 2008.

[38] D. M. Gorinevsky, A. M. Formalsky, and A. Y.-U. Schneider, *Force control of robotics systems*. CRC Press LLC, 1997.

[39] B. Siciliano and L. Villani, *Robot Force Control*, ser. The Springer International Series in Engineering and Computer Science. Springer US, 1999, vol. 540.

[40] J. De Schutter, H. Bruyninckx, S. Dutré, J. De Geeter, J. Katupitiya, S. Demey, and T. Lefebvre, "Estimating first-order geometric parameters and monitoring contact transitions during force-controlled compliant

motion," *International Journal of Robotics Research*, vol. 18, no. 12, pp. 1161–1184, 1999.
[41] J. De Schutter, T. De Laet, J. Rutgeerts, W. Decre, R. Smits, E. Aertbeliën, K. Claes, and H. Bruyninckx, "Constraint-based task specification and estimation for sensor-based robot systems in the presence of geometric uncertainty," *International Journal of Robotics Research*, vol. 26, no. 5, pp. 433–455, 2007.
[42] D. J. Agravante, A. Sherikov, P.-B. Wieber, A. Cherubini, and A. Kheddar, "Walking pattern generators designed for physical collaboration," in *IEEE International Conference on Robotics and Automation*, Stockholm, Sweden, 16-21 May 2016, pp. 1573–1578.
[43] D. J. Agravante, G. Claudio, F. Spindler, and F. Chaumette, "Visual servoing in an optimization framework for the whole-body control of humanoid robots," *IEEE Robotics and Automation Letters*, 2017.
[44] K. Bouyarmane and A. Kheddar, "On weight-prioritized multi-task control of humanoid robots," *IEEE Transactions on Automatic Control*, Cond. accept., revisions submitted.
[45] V. Samy, K. Bouyarmane, and A. Kheddar, "QP-based adaptive-gains compliance control in humanoid falls," in *IEEE International Conference on Robotics and Automation*, Singapore, May 29-June 3 2017.

PLACE PHOTO HERE

Karim Bouyarmane received the double Ingénieur diploma from the École Polytechnique in Palaiseau in 2007 and from the École Nationale Supérieure des Mines de Paris in 2008, and the PhD degree from the University of Montpellier in 2011 after completing the PhD program for full-time in the Joint Robotics Laboratory (JRL) at the National Institute of Advanced Industrial Science and Technology (AIST) in Tsukuba, Japan. He subsequently held a Japan Society for the Promotion of Science (JSPS) postdoctoral fellowship at the Advanced Telecommunications Research Institute International (ATR) in Kyoto, in the Computational Neuroscience Laboratories department, working on brain-robot interfaces. He conducted a CNRS fixed-term contract researcher at the Laboratory of Informatics, Robotics and Microelectronics of Montpellier (LIRMM). He is currently an assistant professor at the University of Lorraine, France.

PLACE PHOTO HERE

Joris Vaillant received the Master degree in interactive systems at Paul Sabatier University, Toulouse, France, in 2010; and the PhD in robotics at the University of Montpellier, in May 2015. He conducted his PhD research at the Interactive Digital Human group at the CNRS-UM Laboratory of Informatics, Robotics, and Microelectronics, Montpellier, France. His research interest is contact planning and whole body motion for humanoids and virtual avatars. He is now working for an SME in Paris, France.

PLACE PHOTO HERE

Kévin Chappellet received the Master degree in computer sciences and applied mathematics (Geometry, Image and CAD) at Joseph Fourier University, Grenoble, France, in 2014. He is working as a research engineer with the Interactive Digital Human (IDH) group at the CNRS-UM Laboratory of Informatics, Robotics, and Microelectronics (LIRMM), Montpellier, France, where he is responsible for the software development and experiments on the HRP-4 humanoid robot. Previously, he was on an internship at the French National Institute for computer science and applied mathematics (INRIA), Grenoble, France. He worked with the IMAGINE group on the calculation of the pressure forces of a garment on a character in a WebGL rendering.

PLACE PHOTO HERE

Abderrahmane Kheddar received the BSCS degree from the Institut National dInformatique (ESI), Algiers, the MSc and PhD degrees in robotics, both from the University of Pierre and Marie Curie, Paris 6. He is presently Directeur de Recherche at the CNRS. He is the Codirector of the CNRS-AIST Joint Robotic Laboratory (JRL), UMI3218/RL, Tsukuba, Japan; and leader of the Interactive Digital Humans (IDH) team at CNRS-UM LIRMM at Montpellier, France. His research interests include humanoid robotics, haptics, and thought-based control using brain machine interfaces. He is a founding member of the IEEE/RAS chapter on haptics (acting also as a senior advisor), the co-chair and co-founding member of the IEEE/RAS Technical committee on model-based optimization, and a member of the steering committee of the IEEE Brain Initiative. He is presently Editor of the IEEE Transactions on Robotics, the Journal of Intelligent and Robotic Systems, and Frontiers in Bionics; he is a founding member of the IEEE Transactions on Haptics and served in its editorial board during three years (2007-2010), he also served as associate editor in the MIT Press Presence journal. He is a member of the National Academy of Technologies of France (NATF), knight in the National Order of Merit, and a Senior Member of the IEEE Society.